EARTHQUAKE ENGINEERING AND STRUCTURAL DYNAMICS, VOL. 26, 701–716 (1997)

POST-EARTHQUAKE RESIDUAL DISPLACEMENTS OF BILINEAR OSCILLATORS

G. A. MACRAE[1]*† AND K. KAWASHIMA[2]‡

[1] *Department of Civil Engineering, University of Washington, Seattle, WA98195-2700, U.S.A.*
[2] *Department of Civil Engineering, Tokyo Institute of Technology, 2-12-1 O-Okayama, Meguro-ku, Tokyo 152, Japan*

SUMMARY

Structures subjected to large inelastic deformations during violent ground shaking do not always return to their initial 'at-rest' position but may have residual displacements. Even if collapse does not occur, large residual displacements may render them unusable or irreparable. In order to investigate the likely magnitude of residual displacement many bilinear single-degree-of-freedom oscillators with specified ductilities of 2·0, 4·0 and 6·0, stiffness ratios ranging from −0·25 to 1·0 and fundamental periods from 0·0 to 3·0 s were subjected to 11 earthquake records from various ground types. It is shown that bilinear oscillators with positive stiffness ratios generally have small residual displacements, while those with negative stiffness ratios tend to undergo little inelastic reversal of deformation and have larger residual displacements. Reasons for this behaviour were able to be explained by means of a 'hysteresis centre curve'. A design example for structures able to be modelled as single-degree-of-freedom oscillators is provided. © 1997 by John Wiley & Sons, Ltd.

Earthquake Engng. Struct. Dyn., **26**, 701–716 (1997)

No. of Figures: 13. No. of Tables: 1. No. of References: 11

KEY WORDS: deflection; design criteria; residual displacement; seismic response

INTRODUCTION

Lifeline structures, including many bridge structures, should not only remain standing but should also be useable after a very large earthquake because, during the time which they cannot be used, society may suffer a tremendous cost and inconvenience. Large residual displacements may make a structure unusable, unsafe, and perhaps irreparable. It is desirable that the likely magnitude of residual displacements be assessable so that existing structures may be retrofitted to avoid undesirable behaviour, and new lifeline structures may be built from structural forms which tend to have low residual displacements.

Riddell and Newmark,[1] as part of a study of the peak response of non-linear systems found that the magnitude of residual displacements may be strongly affected by the hysteresis loop shape. They found that Elastic–Perfectly Plastic (EPP) oscillators sustained plastic deformation predominantly in one direction, bilinear oscillators with a stiffness ratio of 0·05 behaved similarly with slightly more energy dissipation, and oscillators with stiffness degradation absorbed more energy and recovered more than the other oscillators by yielding in both negative and positive directions. The residual displacements of the respective systems with the same period, elastic damping ratio and yield point under the same earthquake record were 22 in (559 mm), 17 in (432 mm), and 5 in (127 mm). Mahin and Bertero[2] found that for some EPP systems, residual displacements averaged more than 40 per cent of the peak displacements and the scatter was large. Residual displacements were found to be smaller for stiffness degrading systems.

* Correspondence to: G. A. MacRae, Department of Civil Engineering, University of Washington, Seattle, WA 98195-2700, U.S.A.
† Assistant Professor
‡ Professor

CCC 0098–8847/97/070701–16$17·50

Received 29 August 1995
Revised 27 August 1996

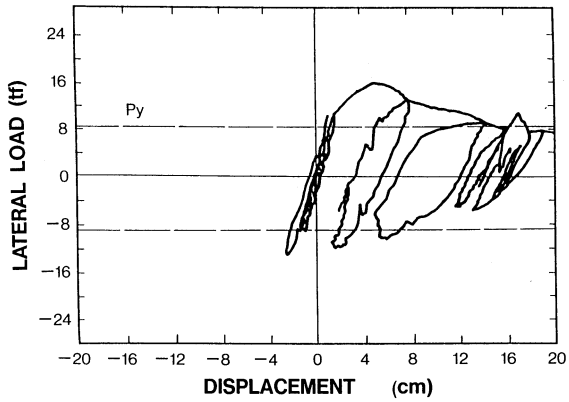

Figure 1. Shaking table behaviour of a model steel bridge pier

Shaking table tests of structures indicate that the magnitude of residual displacement may be related to the material type or structural configuration. For example, some hollow stiffened box-shaped steel bridge piers tested at the Public Works Research Institute (PWRI), Tsukuba, Japan, yielded predominantly in one direction, and the residual displacements were not much smaller than the peak displacements as shown in Figure 1.[3] Shaking table tests of some reinforced concrete structures showed significant yielding occurred in both directions of loading and residual displacements were much lower than the peak displacements,[4] while tests of some base-isolated structures indicated almost no residual displacements at all.[5]

The objectives of this paper are to identify the parameters which control the residual displacements of single-degree-of-freedom bilinear oscillators, to explain why these parameters control, and to develop a method for estimating the residual displacements of single-degree-of freedom structures. This method is then illustrated by an example.

ANALYSIS METHODS

Analytical concept and time-history analysis

Residual displacements were wanted for bilinear oscillators with specified periods, T, stiffness ratios, r (= post-elastic stiffness divided by elastic stiffness), damping ratios, h, and target peak displacement ductilities, μ, subject to several earthquake records.

Oscillators were forced to deform to the specified target peak ductility, μ, using a method similar to that of Meli and Avila[6] for creating inelastic acceleration spectra. In this method an initial estimate of the yield displacement was made and the peak displacement and ductility were calculated by inelastic time-history analysis. Iteration was carried out on the yield displacement until the target peak ductility and the computed peak ductility differed by less than 0·01 per cent. Newmark's linear acceleration method was used for the numerical integration in the time-history analysis. The integration timestep, Δt, was 0·01 s and a unit mass was used for all analyses. The P-delta effect was not included in these analyses.

The values of μ and r able to be used are limited by the displacement stability range of an oscillator. A statically unstable oscillator will deform with no applied force. This occurs when the secant stiffness at the maximum displacement is less than zero as a result of a negative stiffness ratio (i.e. $r < 0{\cdot}0$). The maximum permissible ductility, μ, without instability is given in equation (1):

$$\mu = 1 - \frac{1}{r} \quad (r < 0{\cdot}0) \tag{1}$$

Calculation of residual displacements

There is likely to be a small spring force on the oscillator at the end of a time-history analysis record as the oscillator may still be accelerating. The elastic displacement associated with this spring force must be removed in order to obtain the final residual displacement. If the oscillator is moving elastically along a line shown in Figure 2, where the yield force at the top of the line is H_{yt} and at the bottom is H_{yb}, the residual displacement, d_r, at the end of the analysis is calculated as

$$d_r = \begin{cases} d_\ell, & H_{yb} \leqslant 0{\cdot}0 \leqslant H_{yt} \\ d_L = d_y\left(\dfrac{1-r}{r}\right) & r > 0{\cdot}0 \text{ and either } H_{yb} \geqslant 0{\cdot}0 \text{ or } H_{yt} < 0{\cdot}0 \end{cases} \tag{2}$$

Here d_ℓ is the displacement where the elastic response line at the end of the analysis crosses the zero force line and d_L is the displacement where the post-elastic line intersects the zero force line. If $r < 0{\cdot}0$ and either $H_{yt} < 0{\cdot}0$ or $H_{yb} > 0{\cdot}0$ then the maximum permissible ductility of equation (1) is exceeded and there is no calculation of residual displacement.

Calculation of residual displacement ratio

It is convenient to observe trends in the residual displacements of oscillators with different periods and ductilities subjected to various earthquake motions by non-dimensionalizing the residual displacement. A non-dimensional residual displacement ratio, d_{rr}, which has values ranging from zero to unity was defined, where

$$d_{rr} = | d_r/d_{mr} | \tag{3}$$

Here d_{mr} is the maximum possible residual displacement based on slow unloading from the peak displacement as given in equation (4) and illustrated in Figure 3.

$$d_{mr} = \begin{cases} (\mu-1)(1-r)d_y, & r(\mu-1) < 1 \quad (\text{i.e. } H_{yb}(\mu) < 0{\cdot}0) \\ \dfrac{(1-r)}{r}d_y, & r(\mu-1) \geqslant 1 \quad (\text{i.e. } H_{yb}(\mu) \geqslant 0{\cdot}0) \end{cases} \tag{4}$$

Oscillators analysed

Fifty-one oscillators were analysed with periods ranging from 0·10 s to 0·45 s with a step of 0·025 s, from 0·50 to 1·50 s with a step of 0·050 s, and from 1·60 s to 3·00 s with a step of 0·10 s. The damping ratio, h, was

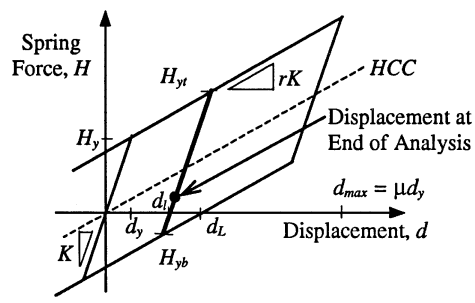

Figure 2. Hysteresis curve with positive stiffness ratio

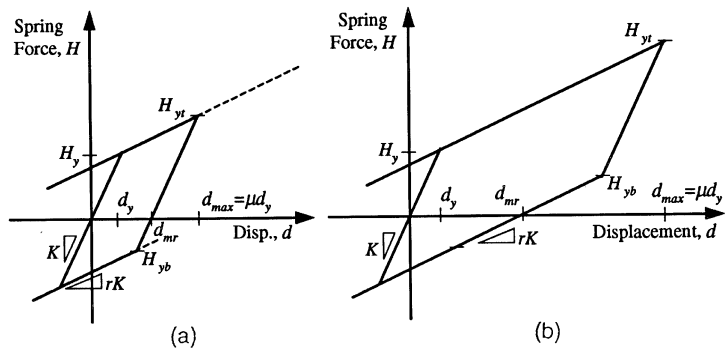

Figure 3. Maximum possible residual displacement, d_{mr}: (a) $r(\mu-1) < 1$; (b) $r(\mu-1) \geqslant 1$

selected to be 2 per cent. Target ductilities of 2, 4 and 6 were used, and the stiffness ratios, r, were $-0{\cdot}25$, $-0{\cdot}10$, $0{\cdot}0$, $0{\cdot}10$, $0{\cdot}25$, $0{\cdot}50$ and $0{\cdot}75$. The ductility, $\mu=6$, exceeded the maximum possible ductility of equation (1) when $r=-0{\cdot}25$ so this combination was not used. There were 20 μ–r combinations for each earthquake record as well as the elastic analysis ($\mu=1$) case.

The eleven earthquake records selected are shown in Table I. A minimum of three earthquake records on each of the three ground types specified in the Japanese Road Bridge Design Specifications[7] were chosen from a report by Kawashima et al.[8] Ground types I–III indicate stiff, medium and soft sites, respectively. An additional 18 s of zero ground motion was added to the end of each earthquake record to enable the oscillators to settle down to elastic vibration for the accurate assessment of residual displacements. Individual acceleration-time graphs and elastic response spectra ($h=2\%$) for each record are given by MacRae and Kawashima.[9]

OVERALL TRENDS OF RESIDUAL DISPLACEMENTS

Residual displacement ratio, d_{rr}, is plotted versus period in Figure 4 for oscillators with various stiffness ratios and a target peak ductility of 4 which were subjected to Record Ia. While d_{rr} depends on period, the average value of d_{rr} over a range of periods did not generally show a strong trend with period. Oscillators with negative stiffness ratios ($r < 0$) had d_{rr} values of almost unity, those with elastic-perfectly plastic loops ($r=0$) had a large amount of scatter and the average d_{rr} was close to $0{\cdot}5$. Those with positive stiffness ratios ($r > 0$) had low residual displacement ratios.

The scatter of residual displacement ratio, d_{rr}, with stiffness ratio, r, for oscillators with a target peak ductility, μ, of 4 subjected to all eleven earthquake records is shown in statistical form in Figure 5. Average (Av), average ± 1 standard deviation (Av $\pm$ sd) and average ± 2 standard deviation (Av $\pm$ 2sd) results are given.

Figure 6 shows d_{rr} for peak ductility levels of μ, of 2, 4, and 6. Here, the average residual displacement ratio is not affected significantly by peak ductility for the larger peak ductilities of 4 and 6. The average values of d_{rr} for a peak ductility level, μ, of 2 were less extreme than for the higher peak ductilities. This may be understood by considering that as the peak ductility becomes small, the hysteresis loop shape may be modelled closely by an elastic perfectly plastic ($r=0$) loop which has average values of d_{rr} close to $0{\cdot}5$.

The records obtained on sites with different ground types made almost no effect on the average residual displacement ratio of oscillators with a target peak ductility, μ, of 4 as shown in Figure 7.

Figure 8 shows the average residual displacement ratios of short and medium period oscillators with a target peak ductility, μ, of 4. Oscillators with fundamental periods of $0{\cdot}1$–$0{\cdot}5$ s, $0{\cdot}55$–$1{\cdot}5$ s and $1{\cdot}6$–$3{\cdot}0$ s were

Table I. Earthquake record characteristics

Record number	Record name	Component	Earthquake name	Date of occurrence	Maximum acceleration (cm/sec^2)	Record duration (sec)	Ground type	Record classification
Ia	Kaihoku Bridge	Transverse	Miyagikenoki	12.06.1978	413·5	38·93	I	302-GR-35
Ib	Kaihoku Bridge	Transverse	Miyagikenoki	20.12.1978	161·3	28·99	I	302-GR-34
Ic	Oita Port	East-West	Ehimeken west coast	21.04.1975	145·3	29·50	I	701-GR-1-2
Id	Kaihoku Bridge	Longitudinal	Miyagikenoki	12.06.1978	363·8	38·89	I	302-GR-35
IIa	Itajima Bridge	Transverse	Oitaken chubu	06.08.1968	615·4	36·67	II	308-GR-4
IIb	Hosojima Port	Transverse	Hyuganada	01.04.1968	302·6	80·00	II	702-GR-1-1
IIc	Ofunato Port	E41S	Miyagikenoki	12.06.1978	226·4	58·00	II	706-GR-2-3
IId	Itajima Bridge	Longitudinal	Ehimeken west coast	06.08.1968	594·5	36·01	II	308-GR-4
IIIa	Kochi Port	Transverse	Hyuganada	01.04.1968	106·6	80·00	III	602-GR-1-1
IIIb	Aomori Port	Transverse	Aomorikenseihooki	16.05.1968	101·1	80·00	III	201-GR-1-2
IIIc	Kinuura Port	Transverse	Gifuken chubu	09.09.1969	84·58	40·50	III	403-GR-1-1

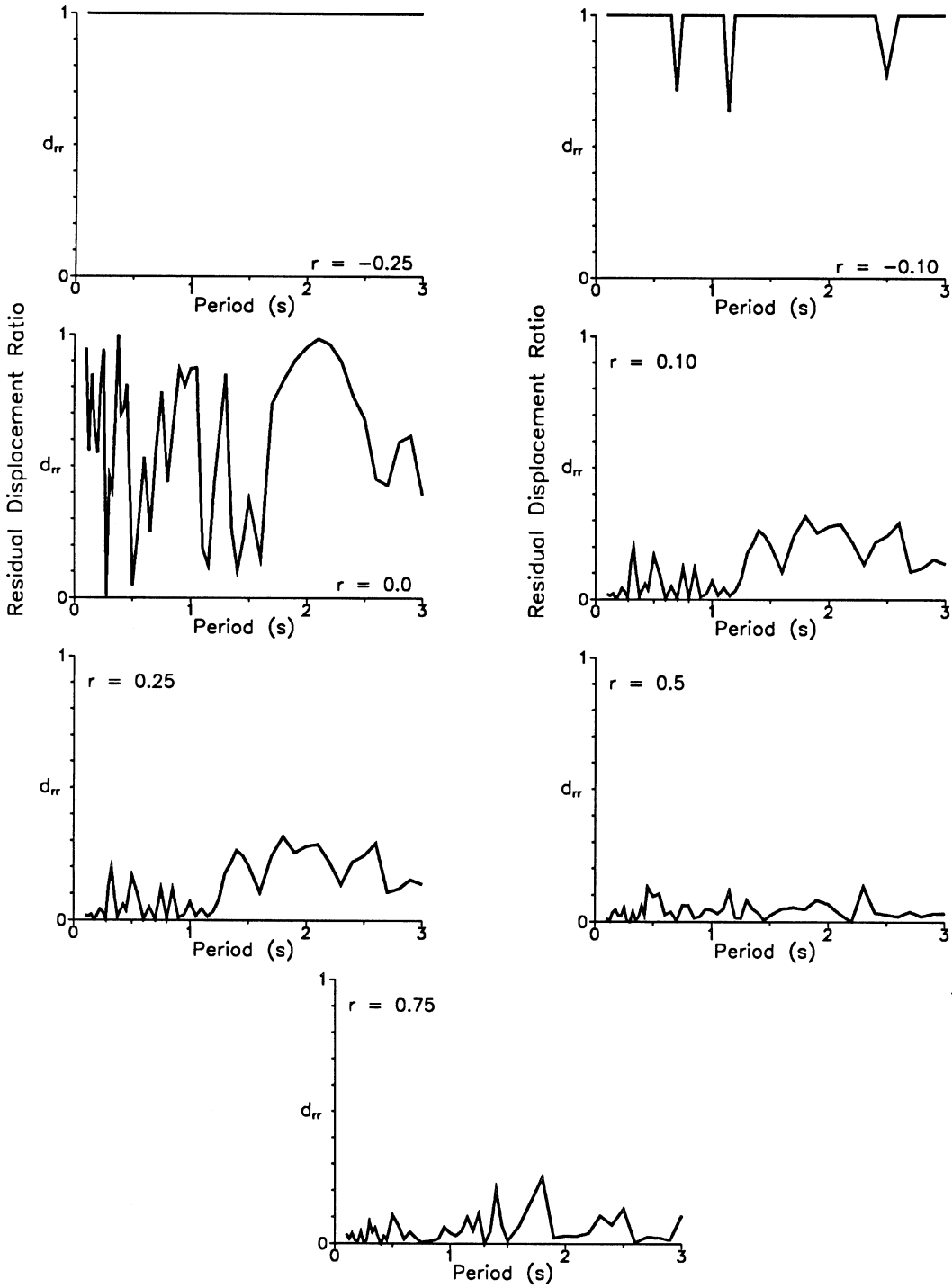

Figure 4. Residual displacement ratio, d_{rr}, versus period, T (Record Ia, $\mu=4$, $h=2$ per cent)

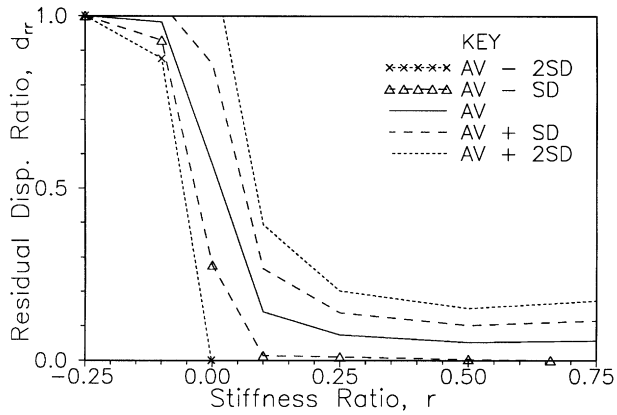

Figure 5. Average residual displacement ratio, d_{rr}, versus stiffness ratio, r, for all records ($\mu=4$)

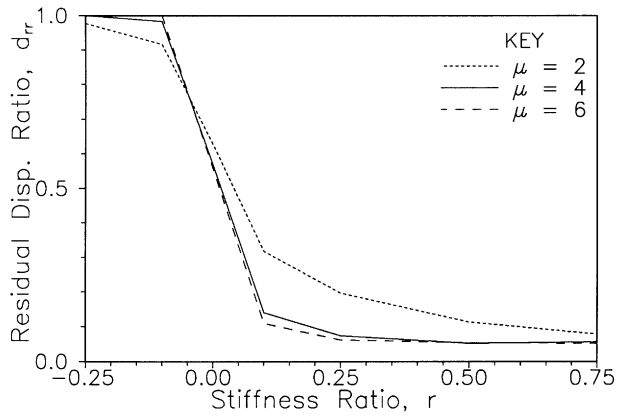

Figure 6. Effect of peak ductility, μ, on average residual displacement ratio, d_{rr}

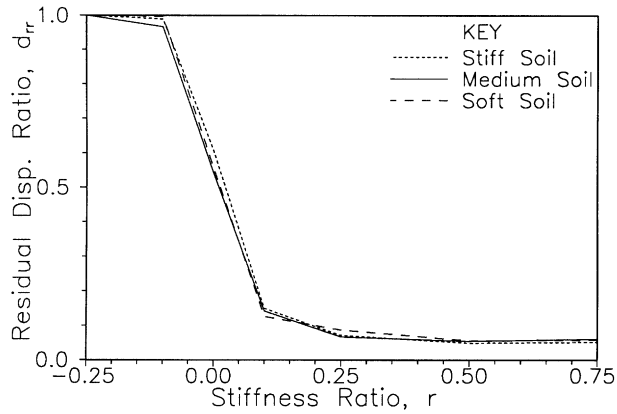

Figure 7. Effect of ground type on average residual displacement ratio, d_{rr} ($h=2$ per cent, $\mu=4$)

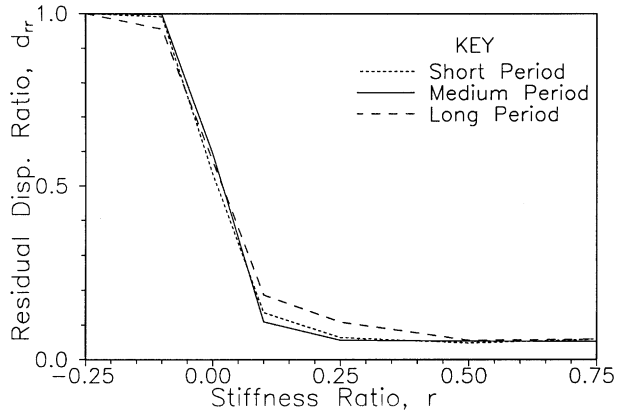

Figure 8. Effect of period, T, on average residual displacement ratio, d_{rr}

defined as short-, medium- and long-period oscillators, respectively. Long-period oscillators with low positive stiffness ratios had average residual displacement ratios slightly greater than those of the shorter period oscillators.

DYNAMIC STABILITY OF INDIVIDUAL OSCILLATORS

Figures 6–8 indicate that the residual displacement ratio, d_{rr}, is significantly more dependent on the stiffness ratio, r, than on the type of earthquake record, oscillator period or peak ductility. Reasons for the dependency on stiffness ratio may be obtained by considering the dynamic stability of individual oscillators as described below.

Figures 9–11 show acceleration ratio versus time, displacement ductility versus time and the hysteretic loops for an oscillator with a period, T, of 1·1 s subjected to Record Ia with stiffness ratios, r, of $-0{\cdot}1$, 0·0, and 0·1. The acceleration ratio is equal to the peak acceleration divided by the yield acceleration. The oscillator with a negative stiffness ratio ($r=-0{\cdot}1$) yielded predominantly in one direction with little inelastic displacement reversal. It had a large residual displacement. The elastic–perfectly plastic ($r=0$) oscillator shown had more inelastic displacement reversal and a lower residual displacement. The oscillator with a positive stiffness ratio ($r=0{\cdot}1$) had a large amount of inelastic displacement reversal and a small residual displacement. All three oscillators tended to oscillate with approximately the same magnitude of acceleration in both the positive and negative directions independently of the shape of hysteresis loop. This is even true for an oscillator with a negative stiffness ratio ($r=-0{\cdot}1$) in which the yield line in only one direction limits the maximum acceleration. Because approximately the same magnitude of acceleration tends to occur in both the positive and negative directions, oscillators tend to yield in the direction where the yield limit is closest to the zero-acceleration (or force) line. The consequences of this behaviour are described below.

Imagine an oscillator oscillating elastically along the line between the upper yield limit, H_{yt}, and the lower yield limit, H_{yb}, in the hysteresis loop with a positive stiffness ratio in Figure 2. It will tend to yield at the lower yield limit, because the point H_{yb} is nearer the zero force line than the upper yield limit and the inertial acceleration (and hence inertial force) is approximately the same in each direction. Yielding will therefore tend to occur toward the zero displacement position. For an oscillator changing direction at the upper yield point, H_{yt}, the velocity will be zero. The potential energy and acceleration will be maximum. When it starts to return to the zero force position its velocity increases. If there are no external forces, the maximum velocity and hence maximum momentum will occur when the lateral inertia load, H, is equal to zero. It will not stop

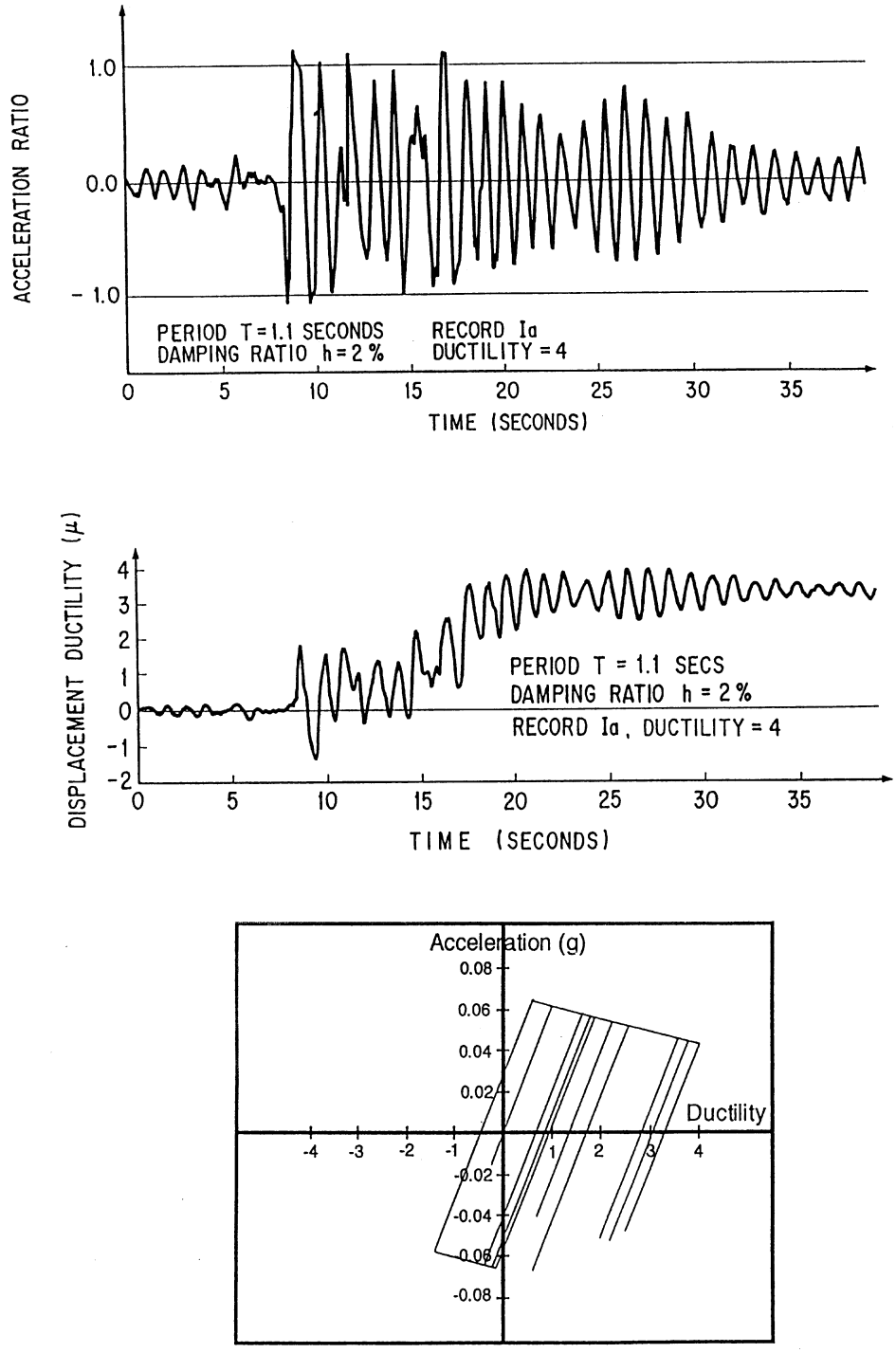

Figure 9. Behaviour of SDOF oscillator with $r = -0{\cdot}10$ ($T = 1{\cdot}1$ s, $h = 2$ per cent, $\mu = 4$)

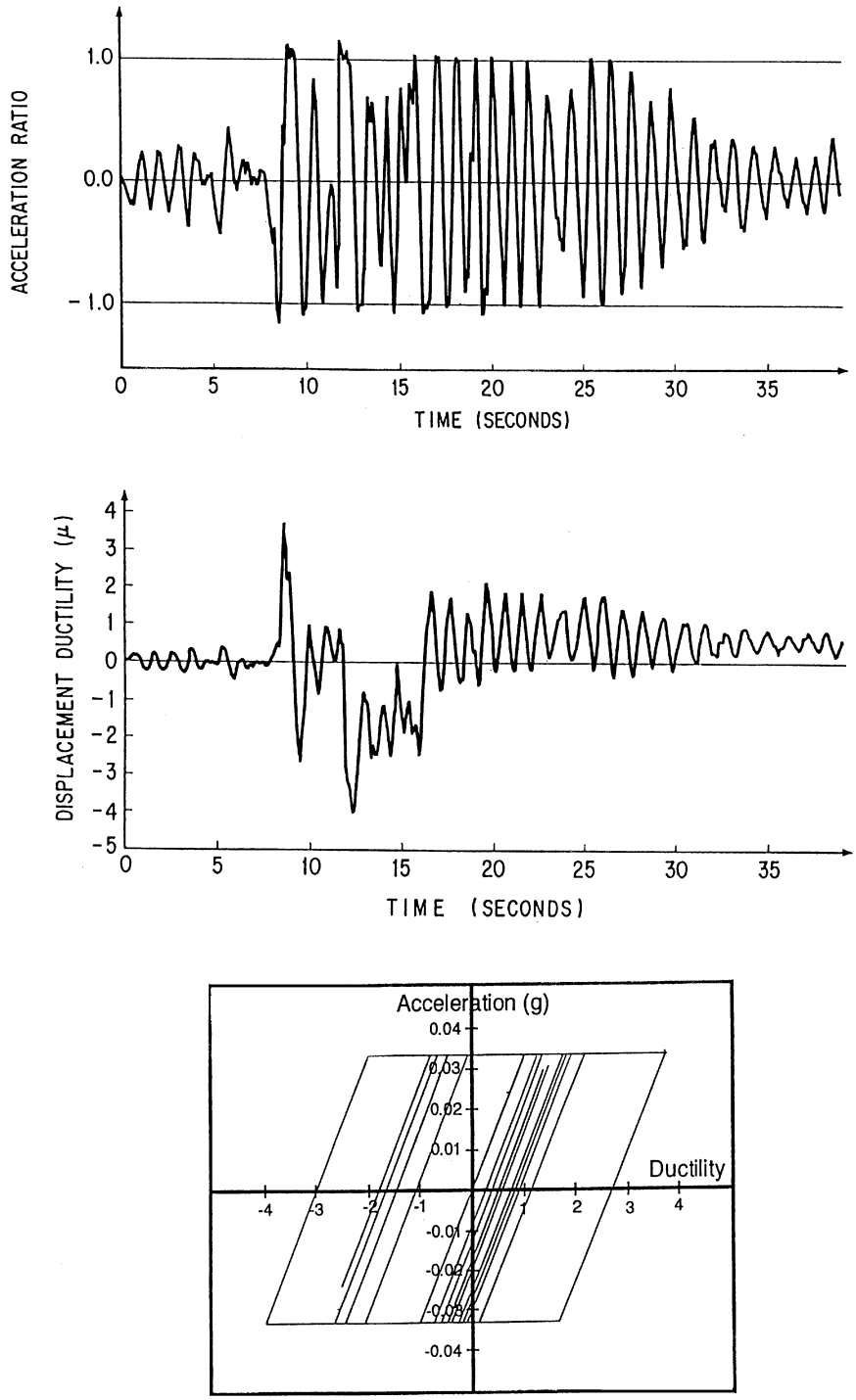

Figure 10. Behaviour of SDOF oscillator with $r=0{\cdot}0$ ($T=1{\cdot}1$ s, $h=2$ per cent, $\mu=4$)

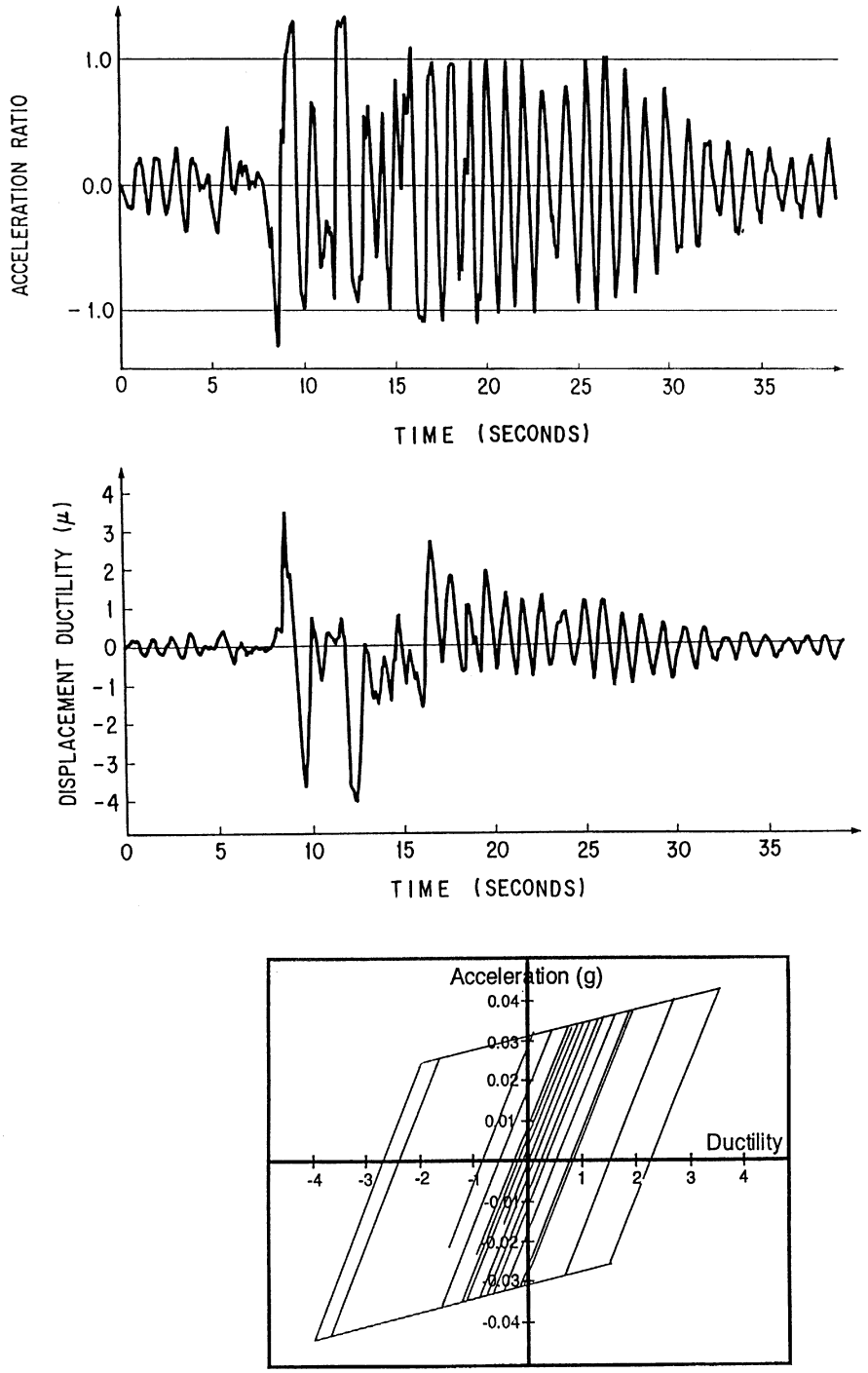

Figure 11. Behaviour of SDOF oscillator with $r=0{\cdot}1$ ($T=1{\cdot}1$ s, $h=2$ per cent, $\mu=4$)

at the displacement corresponding to $H=0$ but will be likely to yield in the direction of the origin thereby reducing the residual displacements as was shown in Figure 11. This loop can be referred to as being 'dynamically stable'.

Elastically–perfectly plastic loops ($r=0{\cdot}0$) always require the same amount of acceleration in each direction in order to yield because the yield limits do not change with displacement. From the elastically–perfectly plastic loop there is no tendency for displacements to occur in one direction. This accounts for the large scatter in the residual displacement ratio for single-degree-of-freedom oscillators with $r=0{\cdot}0$ which was observed in Figure 4.

An oscillator with a negative stiffness ratio and an initially positive displacement oscillating elastically along the line between the upper yield limit, H_{yt}, and the lower yield limit, H_{yb}, will tend to yield at the upper yield limit, H_{yt}, because a lower absolute acceleration is required. It tends to yield away from the zero displacement position. The next time it yields it also will tend to yield in the same direction, away from the zero displacement position. This results in large cumulative residual displacements and little inelastic displacement reversal as was shown in Figure 9. This loop is referred to as being 'dynamically unstable'.

A more general way of describing the stability of hysteresis loops may be obtained using the 'Hysteresis Centre Curve' (HCC) [9]. This method has already been shown to be a suitable means of taking into account the decrease in stability due to the P-Δ effect.[10] For residual displacements too, the HCC concept is useful as it provides a measure of the tendency for oscillators to return to near their initial displacement. A point on the HCC is defined as the mid-point between the upper yield limit, H_{yt}, and the lower yield limit, H_{yb}, on an elastic response line. This is expressed mathematically in equation (5):

$$\mathrm{HCC} = \frac{(H_{yt} + H_{yb})}{2} \tag{5}$$

The full HCC may be obtained by connecting points from many elastic response lines as shown in Figure 2. For bilinear oscillators, the distance between H_{yt}, and H_{yb} is always constant and the HCC is linear with a slope equal to the post-elastic stiffness. If the slope of the HCC is positive, then the oscillator is 'dynamically stable'. For an oscillator with a positive displacement, yielding will tend to occur in the negative direction because the HCC is above the zero acceleration line and the lower yield limit is closest to the zero acceleration line. For an oscillator with a negative displacement, yielding will tend to occur in the positive direction because the HCC is below the zero acceleration line and the upper yield limit is closest. If the slope of the HCC is negative, then the oscillator is 'dynamically unstable'.

Although a bilinear oscillator is assumed here, evaluation of the dynamic stability of oscillators may be extended to those with general hysteresis loop shapes as shown in Figure 12. Consider the behaviour of an oscillator with the force and displacement at point A. The point on the HCC which is intersected by the elastic response line through A is above the zero force line so the lower yield limit is closer to the zero force line than the upper yield limit and yielding is likely to occur toward the initial displacement position. The response is therefore dynamically stable. The degree of stability is related to the secant stiffness, $r_s K$, from the origin to the point associated with A on the HCC as shown in Figure 12. If the secant stiffness ratio, r_s, is negative then yielding is more likely to occur on the upper envelope creating residual displacements and a potential for instability.

As all points on the HCC have a positive secant stiffness ratio, r_s, the whole curve may be defined as being 'unconditionally stable' with the degree of stability reflected in r_s. If the secant stiffness, r_s, is less than zero for all points then the whole loop is 'unconditionally unstable'. A 'conditionally stable' loop is one in which the HCC crosses the line of zero force more than once so the secant stiffness ratio, r_s, may be positive or negative depending on the displacement. Some actual structures have hysteresis loop shapes which change with applied cyclic loading. While they may still be dynamically stable, the secant stiffness should be measured from the revised origin. The behaviour of structures is generally much better with a positive value of r_s than with a negative value.

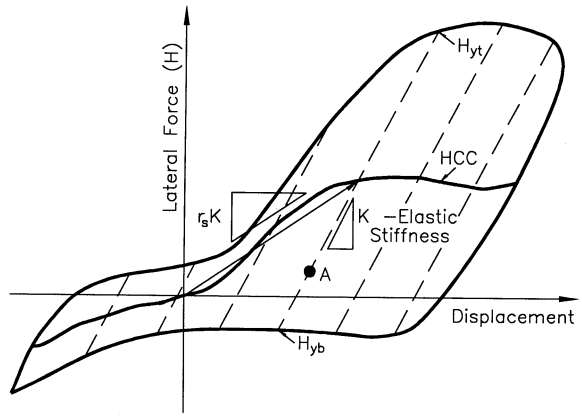

Figure 12. General shaped stable hysteresis curve

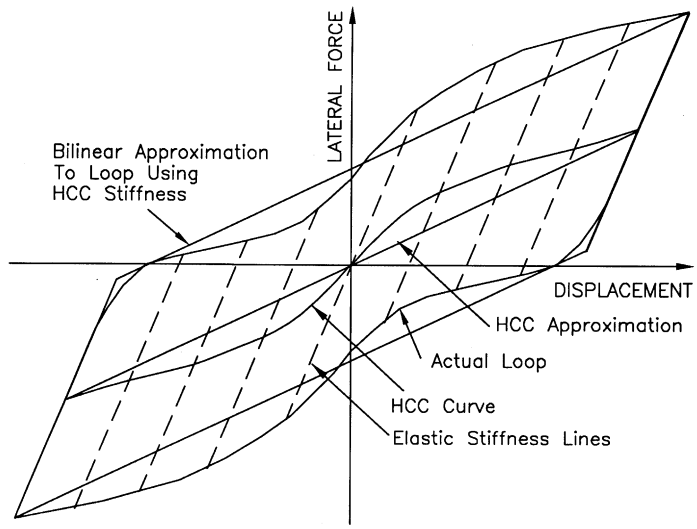

Figure 13. Modelling of general hysteresis loop as bilinear loop to estimate likely residual displacements

DESIGN APPLICATION

A residual displacement prediction procedure may be developed for structures which have properties similar to the bilinear single-degree-of-freedom oscillators analysed here. That is, the hysteresis loop shape should be able to be approximated as a bilinear shape loop and the damping ratio of the elastic structure should be close to 2%. In many cases the hysteretic behaviour may be able to be modelled as bilinear. For example, the hysteresis curve of a reinforced concrete structure during one cycle of loading is able to be modelled by a bilinear curve as shown in Figure 13. Here the post-elastic stiffness of the bilinear curve is set equal to the secant stiffness from the origin to the point on the reinforced concrete HCC corresponding to the peak displacement. The secant stiffness and hence stability of both the reinforced concrete curve and the bilinear curve are therefore the same at the peak displacement. The applicability of the residual displacement prediction method given in the steps below is therefore not limited only to those structures with a bilinear curve.

Step 1: The yield displacement, d_y, of the structure is computed.

Step 2: A best estimate of the maximum expected displacement of the structure, d_{max}, should be obtained. While estimation methods for peak displacements is beyond the scope of this paper it is considered that the method of Priestley *et al.*[11] which uses the equal displacement method for long-period structures, may be reasonable if the oscillator's post-elastic stiffness is positive. The peak ductility, μ, is calculated as d_{max}/d_y.

Step 3: The maximum possible residual displacement, d_{mr}, should be obtained from equation (4) using the known values of μ and r.

Step 4: The likely residual displacement ratio, d_{rr}, should be obtained from Figure 5 for the level of performance required. The *average plus one standard deviation* curve is suggested for a design check.

Step 5: Compute residual displacement, d_r, from equation (3) as

$$d_r = d_{rr}\, d_{mr}$$

If the residual displacement is larger than what is considered to be an acceptable limit, then the structure should be designed to be stronger so that the expected ductility demand is less, or a different lateral load resisting system with a higher stiffness ratio should be used.

As an example a multispan bridge supported by a series of cantilever columns is considered. Isolation devices with bilinear characteristics are placed at the top of each column. The maximum strength of the isolation pads is less than the yield strength of the column. This results in a bilinear lateral force–displacement relationship for the system. The characteristics of a typical isolated column are given below.

Lateral stiffness,	$K = 10\,512$ kN/m (60 kips/in)
Stiffness ratio (equal to the post-elastic stiffness divided by the initial elastic stiffness, K),	$r = 0{\cdot}10$
Height of column from base to centre of weight,	$L = 7{\cdot}315$ m (288 in)
Lateral yield strength,	$H_y = 712$ kN (160 kips)

It is assumed that the structure may be modelled as a single-degree-of-freedom structure and that the predicted peak displacement demand, d_{max}, is 205·8 mm (8·1 in) using rational methods for predicting response. The maximum likely residual displacement is estimated from the steps above as:

Step 1: $d_y = H_y/K = 712$ kN/10 512 kN/m = 67·7 mm (1·72 in)

Step 2: $d_{max} = 205{\cdot}8$ mm (above). $\mu = d_{max}/d_y = 205{\cdot}8$ mm/67·7 mm = 3·04

Step 3: As $r(\mu-1) = 0{\cdot}1\times(3{\cdot}04-1) = 0{\cdot}204$ is less than unity, d_{mr} may be calculated as

$$d_{mr} = (\mu-1)(1-r)d_y = (3{\cdot}04-1)\times(1-0{\cdot}1)\times 67{\cdot}7 \text{ mm} = 124 \text{ mm}(4{\cdot}9 \text{ in}).$$

Step 4: Using the average + one standard deviation (Av + sd) curve for $r = 0{\cdot}10$, the residual displacement ratio, d_{rr}, is obtained from Figure 5 as $d_{rr} = 0{\cdot}27$.

Step 5: The likely residual displacement, $d_r = 0{\cdot}27 \times 124$ mm = 33 mm (1·3 in).

CONCLUSIONS

Residual displacements were obtained from analyses of single-degree-of-freedom bilinear oscillators with 51 different periods, an elastic damping ratio, h, of 2 per cent, stiffness ratios, r, ranging from $-0{\cdot}25$ to 0·75, and

target ductilities, μ, of 2, 4 and 6 to eleven earthquake records. The main findings are:

(1) Bilinear oscillators with negative post-elastic stiffnesses tended to have large residual displacements ratios. They deformed predominantly in one direction. Oscillators with large positive stiffness ratios generally oscillated about the zero displacement position and had smaller residual displacements.
(2) The average residual displacement ratio (a non-dimensional form of the residual displacement) was found to be almost totally dependent on the stiffness ratio of the bilinear curve. The input earthquake record type, period of oscillator and peak ductility do not significantly affect the average values obtained.
(3) Reasons for the dependency of residual displacement ratio on the stiffness ratio were described by means of the 'hysteresis centre curve' (HCC) concept.
(4) A method to model general shaped hysteresis curves as bilinear curves was described, and an example of the estimation of the likely residual displacement of a single-degree-of-freedom structure was provided.

APPENDIX

NOTATION

The following symbols are used in this paper

d	displacement
d_ℓ	point where elastic line crosses zero force line on hysteresis curve
d_L	point where negative yield line intersects zero force line on hysteresis curve
d_{max}	maximum predicted displacement demand
d_{mr}	maximum possible residual displacement
d_r	residual displacement
d_{rr}	residual displacement ratio ($= d_r/d_{mr}$)
d_y	yield displacement
h	elastic damping ratio
H_y	yield force
H_{yb}	force at bottom of elastic line on hysteresis curve
H_{yt}	force at top of elastic line on hysteresis curve
HCC	hysteresis centre curve
K	stiffness
L	height of column
r	stiffness ratio
r_s	secant stiffness ratio
T	period
Δt	timestep
μ	peak displacement ductility

REFERENCES

1. R. Riddell and N. M. Newmark, 'Statistical analysis of the response of nonlinear systems subjected to earthquakes', *Research Report*, University of Illinois, Urbana, Illinois, 1979.
2. S. A. Mahin and V. V. Bertero, 'An evaluation of inelastic seismic response spectra', *J. struct. div. ASCE*, **107**(9) (1981).
3. K. Kawashima, G. A. MacRae, K. Hasegawa, T. Ikeuchi and K. Oshima, 'Ductility of steel bridge Piers from dynamic loading tests', in Y. Fukumoto and G. Lee (eds), *Stability and Ductility of Steel Structures under Cyclic Loading*, CRC Press, Boca Raton, 1992.

4. G. A. MacRae, C. Hodge, M. J. N. Priestley and F. Seible, 'Route 5/405 separation. Shake table tests of as-built and retrofitted configuration', *SSRP Report No. 94/16*, Structural Systems Research Project, Department of Applied Mechanics and Engineering Sciences, University of California, San Diego, 246 pp., 1994.
5. K. Kawashima, K. Hasegawa and H. Nagashima, 'Experiment and analysis on seismic response of menshin bridges', *Proc. 1st US–Japan Workshop on Earthquake Protective Systems of Highway Bridges*, National Centre for Earthquake Engineering Research, Buffalo, New York, U.S.A., 1991.
6. R. Meli and J. A. Avila, 'The Mexico earthquake of September 19, 1985 — analysis of building response', *Earthquake spectra* **5** (1), (1989).
7. Japan Road Association, '*Design Specifications for Road Bridges*, Part V Seismic Design', 1990 (in Japanese).
8. K. Kawashima, K. Aizawa and K. Takabashi, 'Attenuation of peak ground motions and absolute acceleration response spectra', *Report of the Public Works Research Institute*, No. 116, 1985 (in Japanese).
9. G. A. MacRae and K. Kawashima, 'The seismic response of bilinear oscillators using Japanese earthquake records', *J. res. public works res. inst*., Vol. 30, Ministry of Construction, Japan, 1993.
10. G. A. MacRae, '*P*-delta effects on single-degree-of-freedom structures in earthquakes', *Earthquake spectra* **10**, 539–568 (1994).
11. M. J. N. Priestley, F. Seible and E. Calvi, Seismic Design and Retrofit of Bridges, *Wiley*, New York, 1996.

